Suppression of Stimulated Brillouin Scattering in Pulsed Erbium-Doped Fiber Amplifier through Intensity-Modulated Counter-Pumping

Achar V. Harish[1,*]**, Johan Nilsson**[1]

[1]Optoelectronics Research Centre, University of Southampton, UK - SO17 1BJ.

Abstract.   We suppress stimulated Brillouin scattering in an erbium-doped optical fiber amplifier for 50-ns-long transform-limited signal pulses by counter-directional pumping with a pulse burst. The pump pulse burst is codirectional with the parasitic Brillouin Stokes wave, which therefore undergoes cross-phase modulation and thus spectral broadening due to the intensity-modulated pump. The broadening inhibits its growth. We experimentally study the effect of pump pulse parameters and improve the SBS threshold by up to 4 dB when amplifying signal pulses at a wavelength of 1565 nm with pumping at 1536 nm.

Keywords: Stimulated scattering, Brillouin, cross-phase modulation, optical fiber amplifier.

*Achar V. Harish, harish5089@gmail.com

1 Introduction

Stimulated Brillouin scattering (SBS) has the lowest threshold among the nonlinear processes in silica-based fiber amplifiers for narrow-line optical signals, especially for linewidths below the SBS linewidth of a few tens of MHz (including so-called single-frequency light).[1] This limits their power scalability to values below the SBS threshold (or critical power). Above this power the narrow-line signal acts as the "pump" in the SBS process, which thus transfers power from the signal to a parasitizing Brillouin Stokes wave. Methods employed to mitigate SBS and thus increase its threshold include linewidth broadening of the signal by phase-modulation,[2-5] large-mode-area fibers,[6,7] as well as short fibers with high concentrations of laser-active dopants. Other methods broaden the SBS linewidth by varying the strain[8] or temperature along the fiber's length[9] (which may be induced by the laser cycle[10,11]), or by using fibers with special acoustic designs.[12-14] However, none of these approaches is ideal. For example, spectral broadening of the signal is unacceptable for some applications, and quenching limits the concentration to low values for dopants

1

such as erbium.[15–17] Other approaches may be insufficient. Furthermore, if suppression methods are combined, the increase in SBS threshold is often only additive (or less), rather than multiplicative (or better).

In this paper, we demonstrate an alternative option for SBS suppression, wherein a burst of pump pulses broadens the linewidth of the Brillouin Stokes wave in a counter-pumped erbium-doped fiber amplifier (EDFA) for spectrally narrow pulses. Figure 1 illustrates the principle of SBS suppression used in our work. Note that we are broadening the Brillouin Stokes wave instead of the signal. The Stokes wave is broadened by cross-phase modulation (XPM) induced by the optical Kerr effect from the pump since both the pump and Brillouin Stokes wave are traveling in the same direction. The resonant nonlinearity as well as instantaneous heating effects may also add to the phase modulation.[18,19]

Compared to our previous work that dealt with continuous-wave signal and an intensity modulated pump in a Raman fiber amplifier[20,21] the current paper studies several distinct aspects of the SBS suppression scheme in a rare-earth doped pulsed fiber amplifier. The fiber ampifier is now much shorter and the instantaneous signal power is much higher. This necessitates the use of instantaneous pump power which is also much higher, and therefore pulse-burst pumping, to achieve significant XPM of the Stokes wave. Moreover, compared to the cw-case the relative timing of the signal and pump pulse-burst has to be controlled for this scheme to work in a pulsed system. Hence the experimental setup in the present case is relatively more complicated compared to our previous work with cw-signal. We also optimise the pulse-burst pump parameters like the pulse duty cycle and number of pulses within the pulse-burst for best SBS suppression.

Experimentally, we show 4 dB SBS threshold enhancement for 50-ns signal pulses at 1565 nm (transform-limited bandwidth $\sim$10 MHz). It is to be noted that in contrast to earlier work,[22–25] this
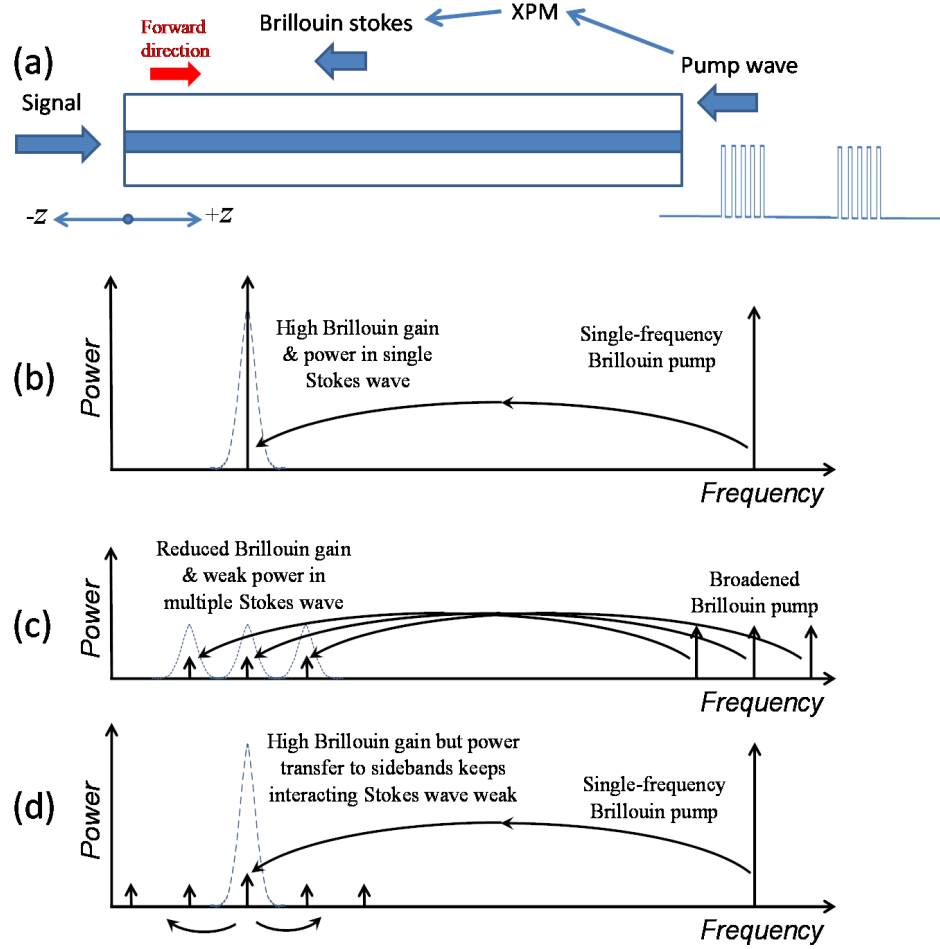
Fig 1 (a) Schematic diagram of an optical fiber showing the signal and the intensity modulated pump wave inducing XPM on the Brillouin Stokes, (b) schematic spectrum of the SBS process showing power transfer from a single-frequency Brillouin pump to a single Stokes line, (c) schematic spectrum of the SBS process showing power transfer from a spectrally broadened Brillouin pump to multiple Stokes lines with reduced Brillouin gain, and (d) schematic spectrum showing the approach used here with a single-frequency Brillouin pump and multiple Stokes lines generated by cross-phase modulation with reduced SBS power transfer due to a reduced interaction with the Stokes wave.

scheme does not use the XPM to broaden the signal (i.e., the Brillouin pump wave) but the Brillouin Stokes wave. Significantly, we believe that the 2.5-times (4 dB) SBS threshold enhancement achieved by the Stokes-wave broadening can remain or even increase when combined with spectral broadening of the signal or Brillouin linewidth.

3

2 Experimental setup

Figure 2 shows our experimental setup for SBS mitigation. Compared to the experimental setup in Ref.,[21] the present setup has several significant changes for producing signal pulses and pulse-burst pumping in EDFA. A fiber-coupled external-cavity tunable laser source (TLS, Agilent 81640A) at 1565 nm with linewidth specified to less than ∼1 MHz is used as a signal seed with 2 mW of output power. The output of the TLS is passed through an isolator, a polarization controller, and a fiber-coupled electro-optic intensity modulator (EOM). This EOM is driven by the first channel of an arbitrary function generator (AFG; Tektronix AFG3252) to produce rectangular signal pulses of 50-ns duration at 20-kHz pulse repetition frequency (PRF). The pulse duration is longer than the phonon lifetime of ∼10 ns in silica for the wavelengths we consider. The period becomes 50 μs, which is much shorter than the erbium fluorescence lifetime of ∼10 ms. The duty cycle becomes 0.1% and the transform-limited linewidth of 50-ns rectangular pulses becomes 10 MHz (FWHM). The average power of the seed is 562 nW and the pulse energy 28.1 pJ. The signal pulses are first amplified in a preamplifier comprising 50 m of Er-doped fiber (EDF). The EDF (Fibercore I-6(980/125)) has a mode-field diameter (MFD) of 5.5 μm, cladding diameter of 125 μm, absorption of 7.3 dB/m at the 1531-nm peak, and numerical aperture of 0.22. An isolator separates the preamplifier from a subsequent main signal-EDFA. The average input signal power to the main signal-EDFA is kept constant at 10 mW, which corresponds to 10 W of peak power at 0.1% duty cycle. The main signal-EDFA, which is our primary focus, comprises 20 m of EDF (Fibercore I-12(980/125)) with numerical aperture of 0.21, MFD of 5.7 μm, cladding diameter of 125 μm, and absorption of 14 dB/m at the peak (1531 nm). Table I lists additional fiber and experimental parameters. The signal transit time through the EDF becomes 100 ns. The EDF is

4

Fig 2 Diagram of our experimental set up. The main amplifier comprises 20 m of erbium-doped fiber (EDF) counter-pumped by a pulse burst for SBS suppression. ISO: Isolator, EOM: Electro-optic modulator, WDM: wavelength division multiplexer, AOM: Acousto-optic modulator.

counter-pumped at a wavelength of 1536 nm. The pump is coupled into, and the residual pump is taken out from, the signal path by 1535/1565 nm fused-fiber wavelength division multiplexers (WDMs). Several 1% taps are connected to the input and output end of the EDF for monitoring the backward (port 14 in Fig. 2) and forward (port 17) output light. A 1% port (16) is also connected to monitor the input pump power. Except for the EDFs, all fibers are standard single-mode fiber (SMF-28 or similar), with effective area of around 85 μm^2.

The 1536-nm seed for the pump is generated by a fiber ring laser with a linewidth of 1-nm. Its output is split into two arms by a 3-dB coupler. The output from one of the arms is boosted in an EDFA to ~0.5 W and then used to pump the signal preamplifier, through a 1535/1565 nm WDM and without any modulation of the pump.

The output from the other arm of the 3-dB coupler was intensity-modulated in an EOM driven by an Agilent 8133A pulse generator and then amplified in an EDFA (AFC). The pump sub-

5

modulation period was between 1 and 20 ns (sub-modulation frequency 50-1000 MHz) and the sub-pulse duration was a fraction of that. The pump pulses were then gated by an acousto-optic modulator (AOM, NEOS N26035) connected to the second channel of the AFG as shown in Fig. 2. This created bursts of typically 1000-4000 pump pulses. The pump duty cycle varied from $\sim$1.8% to $\sim$8%, where a lower duty cycle translates into a higher peak pump power for a given average power. The sub-modulation frequency of the pump was controlled by the pulse generator and the burst duration by the AFG. The AFG also synchronized the bursts with the signal pulses at 20 kHz and controlled their relative timing. The timing of the pump sub-modulation relative to the gating, and thus relative to the signal pulses, was not controlled. The pulse bursts from the AOM were amplified in a power amplifier to boost the average power up to $\sim$1 W, and were then launched into the main signal-EDFA to pump it through a high-power polarization controller (PC). The high-power PC is adjusted to get best SBS suppression in the main signal-EDFA. There, the modulated pump wave broadens the co-propagating Brillouin Stokes wave through XPM and other mechanisms.

In contrast to our previous work on amplification of a continuous-wave (CW) signal in a fiber Raman amplifier,[21] the use of a pulsed signal and the variations of the instantaneous power during the pulse means that the system is no longer perfectly periodic at the sub-modulation PRF. Therefore, the Stokes wave does not broaden into a strictly discrete spectrum. Nevertheless, at least at high sub-modulation PRF, we expect the spectrum will be quasi-discrete with spectral components separated by the sub-modulation PRF. Regardless of the precise details, spectral broadening of the Stokes wave beyond the Brillouin linewidth is expected to reduce the efficiency of the SBS process.

The pump wavelength of 1536 nm is chosen to allow for generation of high-energy pump pulses at high average power as well as for adequate pump absorption in as short EDF as possible.

At shorter wavelengths, the achievable pump energy decreases rapidly, and at longer wavelengths, the absorption decreases rapidly. At 1536 nm, the pump leakage was still significant, 200 mW for 800 mW of launched pump power. The signal wavelength of 1565 nm is chosen to coincide with the gain peak in the main signal-EDFA. With those pump and signal wavelengths, the maximum achievable signal gain per unit length in the main amplifier becomes ∼1.32 dB/m, which corresponds to a minimum effective length of ∼3.30 m. The quantum defect is as small as 1.9%.

For characterization, we used an optical spectrum analyzer (OSA; Advantest Q8384). The time traces were captured with an InGaAs photodetector (Electro-Optics Technology ET-3500F, bandwidth >10 GHz) and an oscilloscope (Agilent Infiniium 54855A, bandwidth 6 GHz). Reported optical powers were measured with power meters. An optical bandpass filter tuned to the peak signal wavelength was used to removed amplified spontaneous emission (ASE) from the signal, pump, and SBS power measurements. The bandpass filter has a bandwidth of 0.5 nm and an excess loss of 1.5 dB, which is compensated for in the reported power data.

The peak signal power may reach up to 1 kW. At this instantaneous power, the nonlinear phase shift (through self-phase modulation, SPM) and the peak Raman gain respectively, reach around 3.78 rad/m and 5.96 dB/m in the EDF in the main amplifier, and around 1.13 rad/m and 1.79 dB/m in SMF-28. The signal is separated from the pump by 120 cm^{-1} (3.6 THz). This is relatively far from the pump's Raman gain peak, and we estimate that the gain is reduced to ∼30% of the peak gain. The peak parametric gain may reach as high as approximately 33 dB/m in the EDF and 9.9 dB/m in SMF-28 (at 1 kW). However, this is only possible for co-directional phase-matched lightwaves. The dispersion of SMF-28 is anomalous and therefore, phase-matching is possible. However, the EDF has normal dispersion , which precludes phase-matching.

7

Table 1 Parameter values for the erbium-doped fiber fibercore I-12(980/125) used in the main signal amplifier.

Parameter	Value
Mode field diameter	5.7 $\mu m^{\dagger}$
Effective area	25.52 μm^2
Fiber core diameter	3.5 $\mu m^{\dagger}$
Fiber core area	9.62 $\mu m^{2\dagger}$
Signal-core overlap Γ	0.526†
Fiber length	20 m ‡
Fiber absorption	14 dB/m @ 1531 nm†
Signal attenuation	0.5 dB/m ‡
Saturation energy at signal wavelength (1565 nm) $(h\nu_s A_{core}(\sigma_e^s + \sigma_a^s)^{-1}\Gamma^{-2})$	11.11 μJ*
Dispersion (D)	-13.1 ps/nm-km @ 1564 nm†

†specified or measured by manufacturer
‡measured by us
*estimated by us

3 Experimental Results

In an initial baseline experiment, we pumped the main signal-EDFA with unmodulated power at

1536 nm. Fig. 3a plots the resulting average output signal power at 1565 nm against the pump

power launched into the main signal-EDFA. The average output signal power increases with pump

power until the average signal output power becomes 200 mW (gain 13 dB) and the peak power

becomes 200 W. Then, the signal starts to roll off due to SBS. Figure 3b shows the growth of the

backscattered SBS power against the launched pump power. The SBS power is measured at the

output of the tap coupler (port 14) and recalculated to the power exiting the EDF. We then switched to burst-pulse counter-pumping of the main signal-EDFA. The temporal shape of the pump bursts is shown in Fig. 4 for the case of sub-modulation at 1 GHz and an intra-burst duty cycle of 90%. Unless stated otherwise, the timing was adjusted so that the pump burst and the signal pulse reach the input end of the main-EDFA at the same time. We used 3000 pump sub-pulses for Fig. 4, for 3-μs burst duration and 5.4% duty cycle. Figure 3a shows the average output signal power plotted against the average launched pump power also for this case. The maximum output power increases by 4 dB, compared to CW pumping, to 500 mW of average output power and 17 dB of gain. This is reached at the maximum pump power of 0.85 W (maximum instantaneous pump power $\sim$15.7 W). We plot the SBS power backscattered from the EDF against the average output signal power in Fig. 3b also for this burst-pumping case. This confirms that SBS is suppressed, relative to CW-pumping. We estimate the effective length L_{eff} for the pump in the EDF to 12 m and thus the maximum nonlinear phase-shift ϕ_{XPM} induced by the pump through XPM to $\phi_{XPM} = (4/3)\gamma L_{eff}P_p = 0.95$ rad. Here, the nonlinear parameter $\gamma = 3.78$ mrad $m^{-1}W^{-1}$ in the EDF. The Raman gain induced by the pump at the signal wavelength and the nearby Brillouin Stokes wavelength is negligible. Figure 5a and 5b show the backward Stokes spectrum at 0.5 W of output signal power with different resolution and wavelength coverage. Figure 5c shows the backward Stokes spectrum for output signal power of 0.2 W and CW pumping. Note that the spectral peaks are a result of SBS. Spectral broadening caused by the pump modulation would not lead to distinct spectral peaks, because of the limited resolution of the OSA. The higher peaks and the cascaded Brillouin Stokes orders confirm that SBS is stronger with CW pumping. Fig. 6 shows the forward signal output spectrum at 0.5 W of output signal power. The spectral background contains approximately 25% of the total output power of $\sim$0.67 W. To repeat, the spectral background is rejected from the measured signal
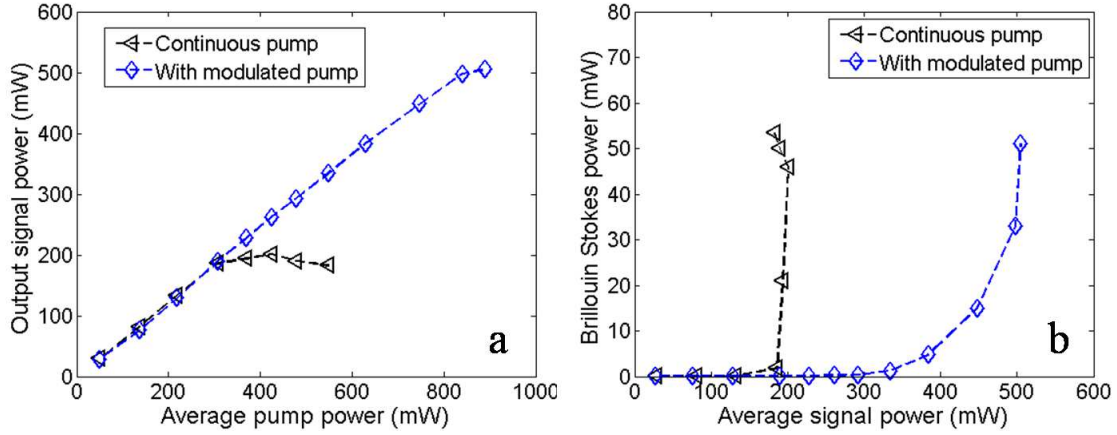
9

Fig 3 Comparison of unmodulated CW pumping and pumping in burst mode with 20 kHz PRF, 1 GHz sub-PRF with 3000 sub-pulses of 0.9-ns duration , (a) average signal output power vs. average launched pump power, (b) SBS backscattered power vs. the average signal output power.

power by a filter.

For this scheme to work effectively, the timing of the signal relative to pump burst, burst duration, sub-modulation frequency, and peak power (or duty cycle) of the pump must be appropriate. We first investigate the effect of the timing of the pump burst relative to the signal pulse. We change the burst pump modulation parameters for this experiment so as to avoid running into other nonlinear effects and still be able to fully explore the relative timing. We keep the sub-modulation frequency constant at 100 MHz, the pump burst duration constant at 2.5 μs (250 sub-pulses), and the average pump power constant at 0.6 W, and vary the timing between the pump burst and signal pulse. The duty cycle of the sub-pulses was adjusted to 90%, which allows for the highest signal power in this case. Figure 7 shows the output signal power as well as the back-scattered SBS power vs. the delay of the pump relative to the signal in the amplifier.

A positive delay means that the signal enters the amplifier earlier than the pump. Note that signal enters the amplifier at the input end and the pump pulse enters the amplifier at the output end. At 0 μs delay, the pump enters the amplifier exactly one transit time of the fiber length before the signal pulse enters. Thus, the leading edge of the pulse exits the amplifier as the leading edge of the

10
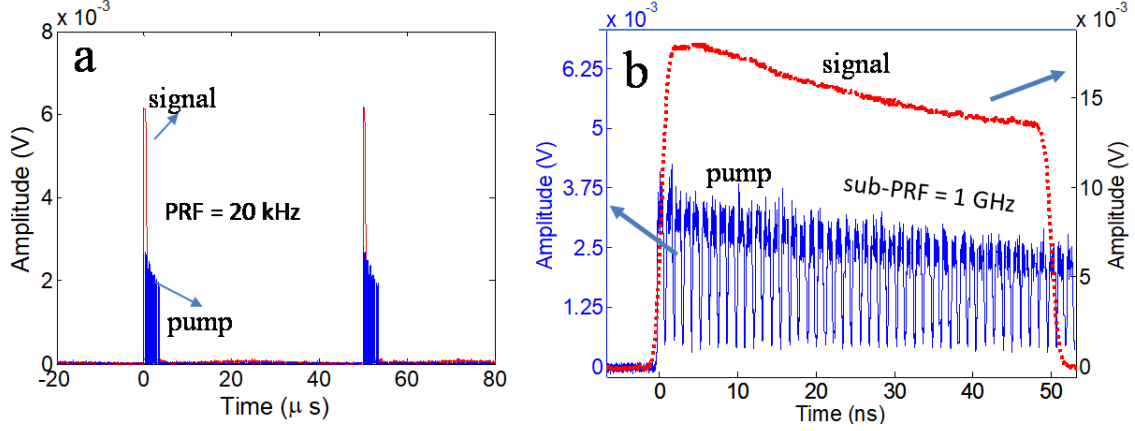
Fig 4 (a) Input pump and signal time traces captured on oscilloscope, (b) zoomed in plot of the time trace in (a). The levels are not to scale.

signal pulse enters it. According to Fig. 7 the output power is lower for positive than for negative delays, pump burst arrives at the input end. This is expected, since the lack of temporal overlap between the pump and signal for positive delays precludes XPM. The maximum signal power in this range is ∼290 mW. The signal power then increases to an overall maximum of 430 mW for a delay of 0 μs. At the same time, the SBS power reaches its overall minimum. For increasing negative delays, the maximum signal power decreases gradually. We attribute this in part to the decrease in pump pulse amplitude within the burst, as exemplified in Fig. 4b. The SBS power in Fig. 7 mirrors the signal power to some extent, although far from perfectly. Furthermore, the variation in SBS power is much lower than that of the signal power. Note also that the signal power is significantly higher even for 4 μs of negative delay than it is for positive delays, even though the pump has then left the fiber before the signal arrives. The reason may be that ASE depletes the gain between pump bursts and cause significant gain modulation even in the absence of signal pulses. In addition, the heat generated by the amplification and pumping processes requires several μs to diffuse out from the core (Fig. 3 in ref.[26]). Note also that although the 1 μs time-step for the delay in the plot is much larger than the signal pulse duration, closer investigations of the delay

11
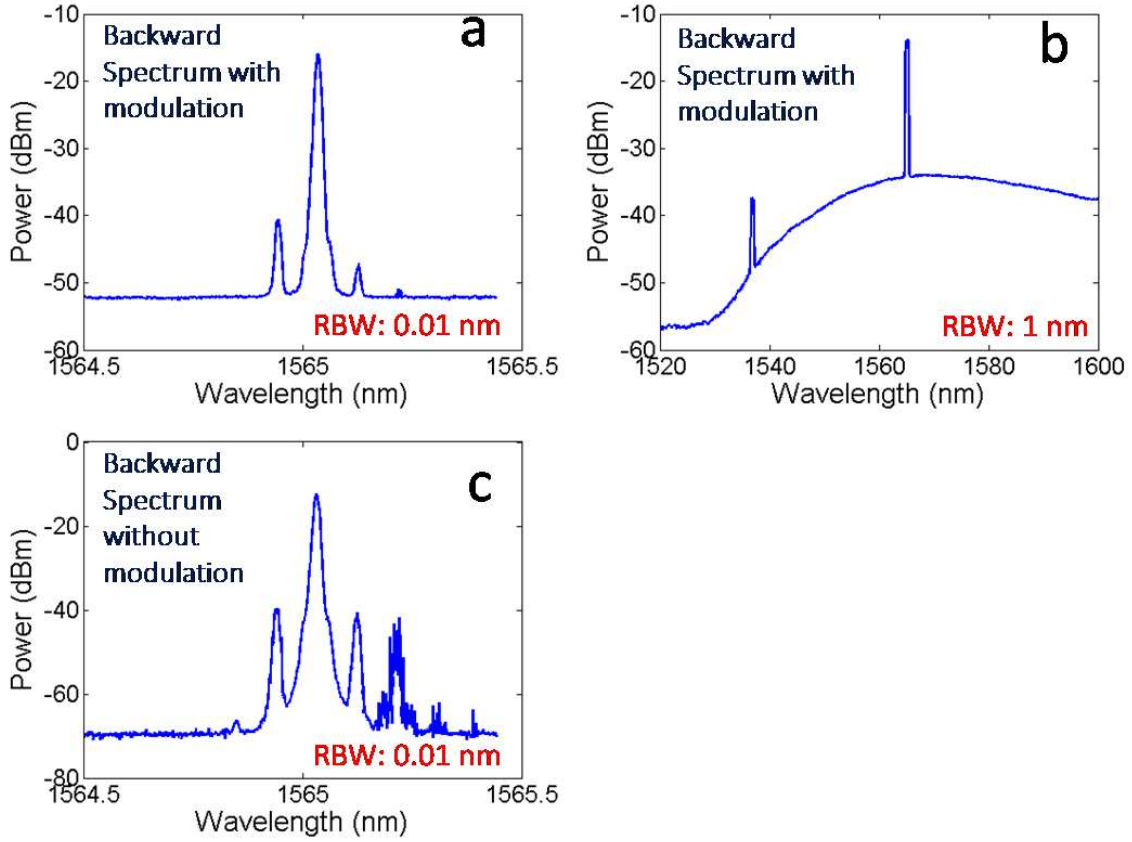
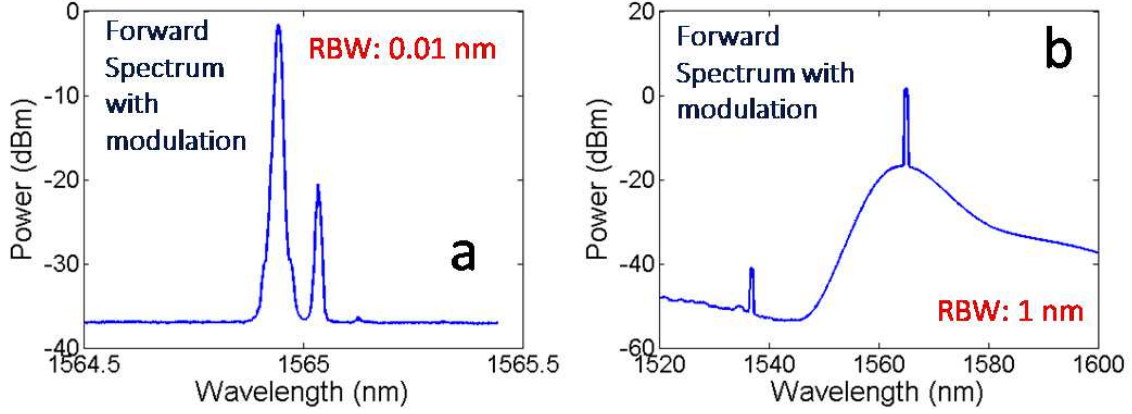**Fig 5** Backward optical Stokes spectrum at 0.85 W of launched pump power in 3-μs burst with 1-GHz sub-PRF and 0.9-ns pump sub-pulse duration. (a) high resolution with resolution bandwidth (RBW) of 0.01 nm, (b) zoomed out plot with lower resolution with RBW of 1 nm, and (c) high resolution spectrum with CW pumping at output signal power of 0.2 W. Note that the further broadening of the Stokes wave caused by the pump modulation is expected to be difficult or impossible to see due to the limited resolution of an optical spectrum analyzer.

did not show any notable deviations from Fig. 7. We also note that it is possible that higher pump power would have allowed for higher output power in Fig. 7. However, the SBS power is already significant and may well be higher than acceptable for many applications.

We also investigated the effect of the sub-modulation frequency of the pump. For this measurement, the average pump power is kept constant at 0.4 W. Figure 8 shows the backscattered Brillouin Stokes power against the sub-modulation frequency of the pump. The burst duration is fixed at 2.5 μs. Starting from 50 MHz, the plot shows a sharp reduction of SBS power with the initial increase in the sub-modulation frequency until 300 MHz and a smaller decrease beyond that.

12

Fig 6 Optical signal output spectrum at 0.85 W of launched pump power in 3-μs burst with 1-GHz sub-PRF and 0.9-ns pump sub-pulse duration. (a) high resolution, (b) zoomed out plot with lower resolution.

Also, we studied the effect of the peak power of the pump on the SBS suppression. In general, the strength of XPM is proportional to the instantaneous peak power of the pulses. However, the pump instantaneous power cannot be arbitrarily increased since it can lead to other nonlinear effects such as SRS and parametric amplification. These can be detrimental if they amplify the parasitic Brillouin Stokes and thus increase the SBS.[21] They can also deplete the pump and thus reduce the erbium gain. In addition, any scattering to wavelengths which are amplified by the erbium-ions also reduces the erbium-gain. Hence the peak power of the pump must be investigated to get good performance. In our setup, the burst duration decides the peak power for a constant average input pump power. Fig. 9a plots the backward output spectrum for different numbers of sub-pulses of the pump in a single burst equivalent to the pump pulse width. With a lower number of sub-pulses, the peak power is high leading to nonlinear spectral broadening as seen in Fig. 9a. This clearly illustrates the importance of the pump peak power and its strong effect on backward-propagating light. We also reiterate that reported SBS powers are measured through a 0.5-nm filter. Fig. 9b plots the output signal power vs the number of sub-pulses of the pump. The sub modulation frequency was 1 GHz, and the average pump power was 0.6 W. We find that
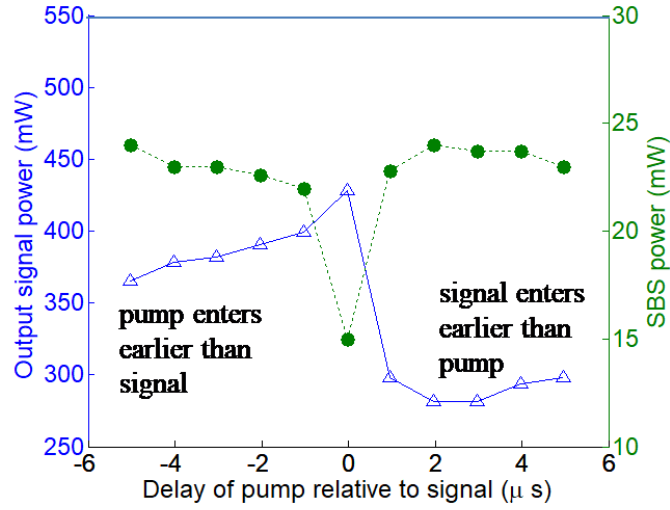
13

Fig 7 Plot of the output signal power (left axis) and backscattered SBS power (right axis) vs. relative timing between signal pulse and pump burst (duration 2.5 μs), with sub-PRF (100 MHz), PRF (20 kHz) and average pump power (0.6 W) kept constant.
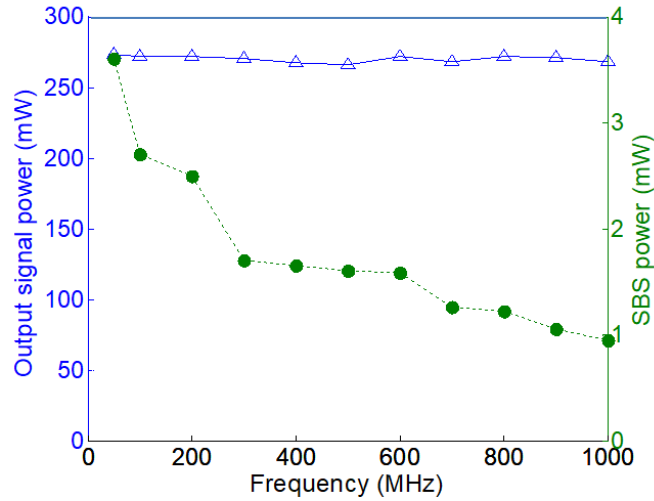

Fig 8 Output signal power (left axis) and backscattered SBS power (right axis) against sub-PRF of the pulses with relative delay of pump and signal , and average pump power kept constant.

the output signal power is indeed decreasing for higher peak powers (number of pump sub-pulses below 3000) which is consistent with the spectrum plotted in Fig. 9a. For lower peak powers, i.e., higher number of pump sub-pulses the output signal power decreases due to SBS. At these peak powers, the modulation of the Stokes wave induced by the pump is not sufficient to check the growth of SBS.

14

It is interesting to consider the difference in nonlinear effects in the forward and backward direction (relative to the signal). The highest peak power is reached for the signal pulses, which therefore might be expected to suffer the strongest nonlinear broadening. However, that is not what we see. One reason for this is the use of backward pumping, which shortens the effective length for the signal. Another possible reason is that the backward-propagating pump only induces parametric gain in the backward direction. Furthermore, in combination with modulated pumping, the practically instantaneous nature of SRS makes it stronger in the co-propagating (backward) direction, despite its intrinsically bi-directional nature. Although the use of a high duty cycle within the burst (e.g., 90%) can make this a small effect, Fig. 4b shows that there are rapid variations on top of the intended modulation. Because the EDF is short the effect of dispersion is small, so any pump modulation slower than the pump-Stokes group delay estimated to 1-10 ps (but faster than the fiber transit time of 100 ns) enhances co-directional SRS relative to counter-directional SRS. We note that we are only able to measure fluctuations down to $\sim$100 ps, so the actual fluctuations may be even larger than shown in Fig. 4b. This further enhances the backward nonlinear scattering relative to the forward scattering, and the lower spectral broadening in the forward direction is another motivation for backward pumping.

4 Discussion

Our experiments show that it is possible to suppress SBS by modulating the pump in erbium-doped fiber amplifiers by at least 4 dB, and we have also explored the influence of some of the parameters. In our previous work,[21] the best SBS threshold enhancement we achieved in the Raman fiber amplifier with modulated Raman pump with cw signal was 4.7 dB. We expect that further investigations of the parameter space, as well as modeling, can lead to further improvements and to
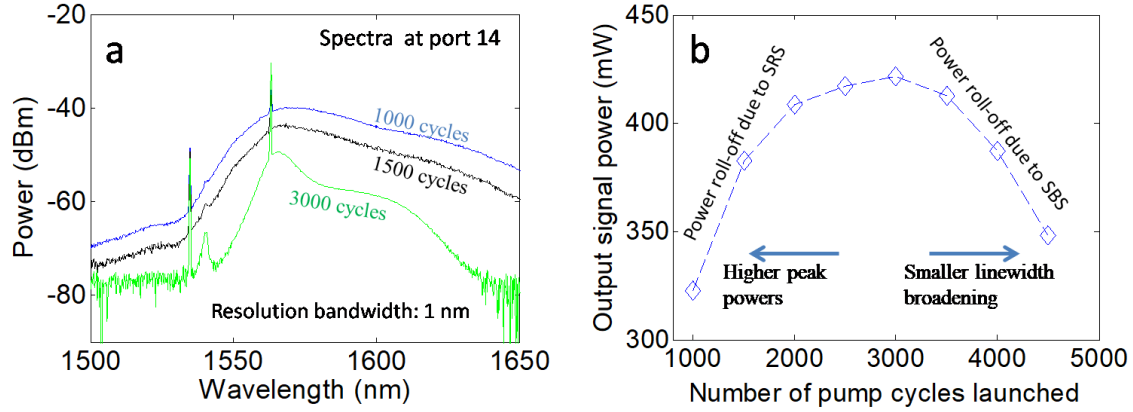
Fig 9 (a) Optical spectra captured with resolution bandwidth of 1 nm at backward output port for different number of pump sub-pulses which corresponds to the pump peak power obtained showing the SRS generated due to high peak powers for smaller number of cycles in the direction of the pump. (b) Plot of average output signal power vs. the number of pump sub-pulses showing the limitation of output power due to SRS at high peak powers and SBS at low peak powers. The sub-PRF is kept as 1 GHz with average pump power of 0.6 W.

better understanding of the importance of different broadening mechanisms in different parameter regimes including signal pule duration, to give one example.

It is also interesting to consider how well pump modulation combines with other methods of SBS suppression. In,[21] we tentatively concluded that combinations perform well in case of a fiber Raman amplifier for a CW signal, because the pump modulation frequency and thus the broadening of the Stokes wave was substantially larger than the Brillouin linewidth. Therefore, other methods which broaden the signal or the Brillouin linewidth could be applied for significant further SBS suppression, although we did not investigate this experimentally. In the present case with a pulsed EDFA, the broadening of the Stokes wave is expected to be more complicated. Further investigations are needed to ascertain the details of this, and how well Stokes-wave broadening combines with other suppression methods.

5 Conclusion

We experimentally suppressed unwanted stimulated Brillouin scattering in an erbium-doped optical fiber amplifier by pumping with a pulse burst. The pump wave is counter-directional with the signal but codirectional with the parasitic Brillouin Stokes wave, which therefore undergoes cross-phase modulation and thus spectral broadening due to the intensity-modulated pump. The broadening inhibits stimulated Brillouin scattering from the signal to the Brillouin Stokes wave. The suppression does not require that the signal is broadened We experimentally studied the effect of selected pulse parameters of a 1536-nm pump and improved the SBS threshold by up to 4 dB when amplifying 50-ns signal pulses at a wavelength of 1565 nm. Further work is needed to fully explore the potential of this approach in fiber amplifiers based on erbium as well as other dopants, in different regimes of operation.

References

1 A. Kobyakov, M. Sauer, and D. Chowdhury, "Stimulated Brillouin scattering in optical fibers," Adv. Opt. Photon., vol. 2, no. 1, pp. 1–59, Dec. 2010.

2 Han-Young Lee, Young-Tak Han, Je-Min Kim, Woo-Seok Yang, Sang Kyu Lim, Chul An, and Hyung-Do Yoon "Effect of external phase modulation on suppression of stimulated Brillouin scattering in an optical transmission system using fiber lasers", Proc. SPIE 4579, Optical Fiber and Planar Waveguide Technology, (19 October 2001).

3 C. Zeringue, I. Dajani, S. Naderi, G. T. Moore, and C. Robin, "A theoretical study of transient stimulated Brillouin scattering in optical fibers seeded with phase-modulated light.," Opt. Express, vol. 20, no. 19, pp. 21196–213, Sep. 2012.

4 A. V. Harish and J. Nilsson, "Optimization of phase modulation with arbitrary waveform generators for optical spectral control and suppression of stimulated Brillouin scattering," Opt. Express, vol. 23, no. 6, p. 6988, Mar. 2015.

5 A. V. Harish and J. Nilsson, "Optimization of phase modulation formats for suppression of stimulated Brillouin scattering in optical fibers," in IEEE Journal of Selected Topics in Quantum Electronics, vol. 24, no. 3, pp. 1-10, May-June 2018, Art no. 5100110.

6 D. Taverner, D.J. Richardson, L. Dong, J.E. Caplen, K. Williams, R.V. Penty, "158 μJ pulses from a single transverse mode, large mode-area EDFA," Opt. Lett., 22 (1997), pp. 378-380.

7 S. Höfer, A. Liem, J. Limpert, H. Zellmer, A. Tünnermann, S. Unger, S. Jetschke, H.-R. Müller, and I. Freitag, "Single-frequency master-oscillator fiber power amplifier system emitting 20 W of power," Opt. Lett. 26, 1326-1328 (2001).

8 N. Yoshizawa and T. Imai, "Stimulated Brillouin scattering suppression by means of applying strain distribution to fiber with cabling," J. Light. Technol., vol. 11, no. 10, pp. 1518–1522, 1993.

9 Y. Imai, N. Shimada, "Dependence of stimulated Brillouin scattering on temperature distribution in polarization-maintaining fibers", IEEE Photon. Technol. Lett., vol. 5, pp. 1335-1337, Nov. 1993.

10 Y. Jeong, J. Nilsson, J. K. Sahu, D. B. Soh, C. Alegria, P. Dupriez, C. A. Codemard, D. N. Payne, R. Horley, L. M. B. Hickey, L. Wanzcyk, J. Chryssou, J. A. Alvarez-Chavez, and

P. W. Turner, "Single-frequency single-mode plane-polarized ytterbium-doped fiber master-oscillator power amplifier source with 264 W output power", Opt. Lett. 30, 459-461 (2005).

11 V. I. Kovalev and R. G. Harrison, "Suppression of stimulated Brillouin scattering in high-power single-frequency fiber amplifiers," Opt. Lett. 31, 161-163 (2006).

12 C. Vergien, I. Dajani, and C. Robin, "18 W single-stage single-frequency acoustically tailored Raman fiber amplifier," Optics Letters, vol. 37, no. 10. p. 1766, 2012.

13 P. D. Dragic, C.-H. L. C.-H. Liu, G. C. Papen, and A. Galvanauskas, "Optical fiber with an acoustic guiding layer for stimulated Brillouin scattering suppression," (CLEO). Conf. Lasers Electro-Optics, 2005., vol. 3, 2005.

14 S. Yoo, C. A. Codemard, Y. Jeong, J. K. Sahu, and J. Nilsson, "Analysis and optimization of acoustic speed profiles with large transverse variations for mitigation of stimulated Brillouin scattering in optical fibers", Appl. Opt. 49, 1388-1399 (2010)

15 M. Shimizu, M. Yamada, M. Horiguchi, E. Sugita, "Concentration effect on optical amplification characteristics of Er-doped silica single-mode fibers", IEEE Photon. Technol. Lett., vol. 2, pp. 43-45, 1990.

16 P. Blixt, J. Nilsson, T. Carlnäs, and B. Jaskorzynska, "Concentration dependent upconversion in Er3+-doped fiber amplifiers: experiments and modeling", IEEE Photonics Technol. Lett. 3, 996-998 (1991)

17 E. Delevaque, T. Georges, M. Monerie, P. Lamouler, J.-F. Bayon, "Modeling of pair-induced quenching in erbium-doped silicate fibers", IEEE Photon. Technol. Lett., vol. 5, pp. 73-75, Jan. 1993.

18 Y. Feng, B. M. Zhang, and J. Nilsson, "Numerical Analysis on the Influence of Photo Darkening Heating Induced Phase Distortion on Fiber Coherent Combining CPA Scheme," in Conference on Lasers and Electro-Optics, OSA Technical Digest (online) (Optical Society of America, 2018), paper JTh2A.110.

19 Y. Feng, B. M. Zhang, A. Harish, and J. Nilsson, "Thermally Induced Distortions of the Temporal Phase Of Optical Pulses In Phosphorous-doped Silica Fibers," in Advanced Solid State Lasers, 2015, p. AM5A.19.

20 A.V. Harish and Johan Nilsson, "Suppression of stimulated Brillouin scattering in a counter-pumped fiber Raman amplifier with intensity modulated pump", Proc. Europhoton 2018, paper FrM1.6

21 A.V. Harish and J. Nilsson, "Suppression of stimulated Brillouin scattering in fiber Raman amplifier through pump modulation," Journal of Lightwave Tech. 2019 (accepted).

22 F. H. Tithi and M. S. Islam, "Suppression of stimulated Brillouin scattering effect using nonlinear phase modulation," Int. Conf. Electron. Comput. Eng. (ICECE 2010), no. December, pp. 135–138, 2010.

23 S. S. Lee, H. J. Lee, W. Seo, and S. G. Lee, "Stimulated brillouin scattering suppression using cross-phase modulation induced by an optical supervisory channel in WDM links," IEEE Photonics Technol. Lett., vol. 13, pp. 741–743, 2001.

24 Y. Horiuchi, S. Yamamoto, and S. Akiba, "Stimulated Brillouin scattering suppression effects induced by cross-phase modulation in high power WDM repeaterless transmission," Electron. Lett., vol. 34, no. 4, p. 390, 1998.

25 G. Ravet, A.F. Fotiadi, M. Blondel, and P. Megret, "Suppression of Stimulated Brillouin scat-

tering with a Raman Fiber Amplifier," in Proceedings Symposium IEEE/LEOS Benelux Chapter, Ghent, 2004, pp. 199–202.

26 M. K. Davis, M. J. F. Digonnet, and R. H. Pantell, "Thermal effects in doped fibers," J. Lightwave Technol., vol. 16, no. 6, pp. 1013–1023, 1998.

A.V. Harish received his doctorate from Optoelectronics Research Centre (ORC), University of Southampton, United Kingdom, in 2017. He has worked on optical fiber amplifiers, non-linear fiber optics at ORC and non-destructive testing with optical fiber sensors at IIT-M. His current research interests are suppression of stimulated Brillouin scattering in high power optical fiber amplifiers, mitigation of thermal mode instability in fiber lasers, and non-destructive testing of structures using fiber Bragg gratings.

Johan Nilsson is a Professor at the ORC, University of Southampton, UK, and head of the High Power Fiber Lasers research group. In 1994, he received Ph.D. in Engineering Science from the Royal Institute of Technology, Stockholm, for research on optical amplification. Since then, he has worked on optical amplifiers and amplification in lightwave systems, optical communications, and guided-wave lasers, first at Samsung Electronics and later at ORC. He has published some 400 scientific articles.

List of Figures

5   Backward optical Stokes spectrum at 0.85 W of launched pump power in 3-μs burst with 1-GHz sub-PRF and 0.9-ns pump sub-pulse duration. (a) high resolution with resolution bandwidth (RBW) of 0.01 nm, (b) zoomed out plot with lower resolution with RBW of 1 nm, and (c) high resolution spectrum with CW pumping at output signal power of 0.2 W. Note that the further broadening of the Stokes wave caused by the pump modulation is expected to be difficult or impossible to see due to the limited resolution of an optical spectrum analyzer.

6   Optical signal output spectrum at 0.85 W of launched pump power in 3-μs burst with 1-GHz sub-PRF and 0.9-ns pump sub-pulse duration. (a) high resolution, (b) zoomed out plot with lower resolution.

7   Plot of the output signal power (left axis) and backscattered SBS power (right axis) vs. relative timing between signal pulse and pump burst (duration 2.5 μs), with sub-PRF (100 MHz), PRF (20 kHz) and average pump power (0.6 W) kept constant.

8   Output signal power (left axis) and backscattered SBS power (right axis) against sub-PRF of the pulses with relative delay of pump and signal , and average pump power kept constant.

9   (a) Optical spectra captured with resolution bandwidth of 1 nm at backward output port for different number of pump sub-pulses which corresponds to the pump peak power obtained showing the SRS generated due to high peak powers for smaller number of cycles in the direction of the pump. (b) Plot of average output signal power vs. the number of pump sub-pulses showing the limitation of output power due to SRS at high peak powers and SBS at low peak powers. The sub-PRF is kept as 1 GHz with average pump power of 0.6 W.

List of Tables

24